The Heme Iron Coordination Complex in His64(E7)Tyr Recombinant Sperm Whale Myoglobin†

Serge Pin* and Bernard Alpert

Laboratoire de Biologie Physico-Chimique, Université Paris VII, 2 place Jussieu, 75251-Paris Cedex 05, France

Robert Cortès and Isabella Ascone

Laboratoire pour l'Utilisation du Rayonnement Electromagnétique (LURE), Université Paris XI, Batiment 209, 91405-Orsay Cedex, France

Mark L. Chiu and Stephen G. Sligar*

School of Chemical Sciences and Beckman Institute for Advanced Science and Technology, University of Illinois, Urbana, Illinois 61801

Received June 20, 1994®

ABSTRACT: By using site-directed mutagenesis of recombinant sperm whale (SW) myoglobin, the native distal histidine residue, at position 64 (the helical position E7), has been replaced with a tyrosine. The mutation of His64Tyr SW myoglobin has an analogous heme iron electronic structure as that of native hemoglobins M Boston and M Saskatoon. Optical spectroscopy showed that the distal tyrosine bound to the heme iron had a p*K* value of 5.6. In the pH range of 4.7–11.0, electron spin resonance spectroscopy suggested the presence of two heme iron ligation schemes: the heme iron bound to a distal water molecule or to a distal tyrosine residue. The heme iron coordination in the wild-type myoglobin and in the His64Tyr SW Mb mutant was studied by X-ray absorption near-edge structure (XANES) spectroscopy. Indeed, the heme iron K-edge reflects the electronic organization of the metal inside the six-coordinated complex. Comparative analysis of X-ray absorption heme iron K-edge shapes showed that the heme iron of His64Tyr SW myoglobin is bound to the oxygen atom from the phenol group of the distal tyrosine residue (Fe–OH_Φ). When the pH value decreased from pH 7 to 5.6, the Fe–OH_Φ bond strength decreased, resulting in an increase of the heme iron high-spin population of His64Tyr SW myoglobin. At low pH values, the Fe–OH_Φ bond can be disrupted with the possibility of heme iron binding of another ligand having a higher affinity. When the heme Fe–OH_Φ interaction was strong in His64Tyr SW myoglobin, the heme iron was bonded to the oxygen atom of the phenol group of tyrosine without displacement of the hydrogen atom of the phenol group.

The iron chemistry of heme proteins is controlled by the ligands bound to the heme iron. Typically, the heme group iron has four conserved protoporphyin IX pyrrole nitrogen ligands. In addition, the heme iron can have one or two more ligands which could either be an endogenous residue (such as histidine, methionine, or cysteine, etc.) or be an exogenous solution molecule (such as cyanide, water, carbon monoxide, etc.). The differences in the heme iron's ability to perform different kinds of chemistry depend on the nature of the heme iron ligands. A review of the different classes of heme proteins has been made (Palmer, 1979; Peisach *et al.*, 1971). The strength of the heme iron–ligand bond has been proposed to distinguish an oxygen binding protein from an oxygenase or a peroxidase (Choi & Spiro, 1983; Spiro *et al.*, 1979; Spiro, 1983). Changes of the heme ligands of cytochrome b_5 (Sligar *et al.*, 1987), sperm whale myoglobin (SW Mb), and cytochrome *c* (Raphael & Gray, 1991) can alter that heme iron's coordination chemistry. Complete gene syntheses of cytochrome b_5 (Beck von Bodman *et al.*, 1986) and SW Mb (Springer & Sligar, 1987) permit the facile construction of mutant proteins with altered axial ligand–heme coordination schemes.

We have extended our analysis of the His64Tyr SW Mb mutant. This tyrosine–histidine heme iron coordination has been shown to be analogous to Hb M Boston and M Saskatoon by optical absorption, electron spin resonance, and resonance Raman spectroscopies (Egeberg *et al.*, 1990). The conclusions regarding the nature of the heme iron coordination have been based on the crystallographic structures of these Hb M mutants which show that the phenolate group of tyrosine is coordinated to the heme iron (Pulsinelli *et al.*, 1973). In this paper, we examined the heme iron coordination state of the His64Tyr SW Mb mutant by monitoring the optical absorption, electron spin resonance (ESR), and X-ray absorption near-edge structure (XANES) spectroscopies at different pH values.

This mutant was screened initially with optical absorption and ESR spectroscopies. Visible absorption of the His64Tyr SW Mb mutant showed absorption bands at 486 and 600 nm. Since these bands were distinct from the bands present for the aquometmyoglobin (535 and 635 nm), they were assigned to the His/Tyr heme iron coordination sphere, and they were used to monitor the properties of the heme iron–tyrosine bond. ESR of high-spin metMb also characterizes the heme iron coordination state. His64Tyr SW Mb spectra have rhombically split high-spin heme iron signals with *g* values of 6.63, 5.31, and 1.98 at pH 7.0. Since wild-type Mb has heme iron signals at 6.0 and 2.0, the *g* values of 6.63 and 5.31 were used to characterize the different heme iron ligands during changes in pH. We have focused on the heme iron coordination changes at pH values less than pH 8.3.

† This work was supported in part by NIH Grant GM37755, NIH Grant GM31756 (S.G.S.), and Institut Curie Contrat de Recherche Coopératif (S.P. and B.A.).

* To whom correspondence should be addressed.

® Abstract published in *Advance ACS Abstracts,* September 1, 1994.

0006-2960/94/0433-11618$04.50/0

The sensitivity of XANES spectroscopy was used to detect subtle iron electronic differences in hemoglobin and myoglobin (Pin *et al.*, 1982; Bianconi *et al.*, 1985; Amiconi *et al.*, 1989; Penner-Hahn & Hodgson, 1989). This technique permits investigation of the structural and electronic properties of the heme iron coordination complex. Indeed, XANES spectroscopy distinguishes the binding of different ligands, the heme iron oxidation state (Morante *et al.*, 1983; Pin *et al.*, 1986), and the heme iron spin equilibrium states (Morante *et al.*, 1983; Oyanagi *et al.*, 1987; Pin *et al.*, 1989). This study assessed and compared the structural and electronic properties of the heme iron coordination complex of wild-type and His64Tyr recombinant myoglobins.

MATERIALS AND METHODS

Myoglobin Preparation. Native myoglobin solutions were prepared from lyophilized sperm whale myoglobin purchased before the ban. The His64Tyr SW Mb mutant was prepared and purified as previously described (Springer & Sligar, 1987; Egeberg *et al.*, 1990). Electrospray mass ionization spectrometry confirmed the correct expression of the SW Mb mutation (Charles Edmonds, personal communication).

Optical Spectroscopy. Optical spectra of 10 μM solutions of His64Tyr SW Mb in 0.1 M potassium phosphate, pH 5–13, and 0.1 M sodium acetate, pH 3–5, were recorded on Hewlett-Packard 8450A and Varian 219 UV/visible spectrophotometers. Each pH measurement represented a separate sample prepared for the specific pH range. Each phosphate buffer was made by mixing solutions of 0.1 M monobasic and dibasic potassium phosphate solutions. The high-pH phosphate buffers were made by mixing 0.1 M dibasic and tribasic potassium phosphate solutions. Each sample was allowed to equilibrate for at least 1 h at room temperature. The average of the absorbance values of 750 and 800 nm was used as a background value which was then subtracted from the entire spectrum. The absorbance values at 410, 486, 542, and 600 nm were normalized to the absorbance value at 280 nm.

The titration data were fit to the Henderson–Hasselbach equation (Stryer, 1988) using a Levenberg–Marquardt algorithm (Press *et al.*, 1986):

$$\log \frac{1-f}{f} + pK = pH \quad (1)$$

$$f = \frac{A - A_{initial}}{A_{final} - A_{initial}} \quad (2)$$

where f is the fraction of metMb species with a disrupted heme iron–tyrosine bond, A_{final} is the absorbance value of the metMb complex with the intact heme iron–tyrosine bond at high pH values, and $A_{initial}$ is the initial absorbance value of the metMb without the heme iron–tyrosine bond at low pH values.

Electron Spin Resonance Spectroscopy. Electron spin resonance (ESR) spectroscopy of 400 μM Mb solutions was performed on a Bruker ESR 220D-SRC with a modulation frequency of 100 kHz, a modulation amplitude of 2 G, a power of 4 mW, and a spectral width of 4000 G collected over 1024 points at 7 K equipped with a Bruker microwave bridge ER-4MRH, liquid helium dewar, a Varian gauss meter, and an EIP microwave 548A frequency meter. Each ESR measurement represented a sample that was prepared separately in its respective buffered solution. Data manipulation on a PC employed a user-modified EWARE program (Morse, 1987).

X-ray Absorption Study. X-ray absorption experiments were carried out with synchrotron radiation from the DCI electron storage ring of LURE (Orsay, France) with a positron beam energy of 1.85 GeV and a maximum stored current of 310 mA. The experiments were performed on the EXAFS II setup with a Si (311) monochromator. Harmonics were rejected by using a grazing incident mirror with the cutoff at 10 keV. The heme iron K-edge measurements were made by the total fluorescence emission of the iron as a function of incident X-ray energy (Jaklevic *et al.*, 1977, 1987). A plastic scintillation detector (Tourillon *et al.*, 1990), in front of which a 15 μm Mn filter was set, was placed at 90° from the incident beam in the horizontal plan to record the fluorescent intensity from the sample. In the experimental conditions used, the band resolution at full width at half-maximum given by the monochromator slits was 1.3 eV. The myoglobin samples of less than 1 mL in a Teflon cell enclosed by a 6 μm mylar film were maintained at 19 °C. The viability of the samples was checked by similarities of the optical spectra recorded before and after XANES measurements with a Cary Model 219 spectrophotometer.

Each XANES spectrum was averaged over at least five scans. Each XANES scan was collected with a 0.2 eV step and a 5 s integration time in the 7090–7160 eV range. In addition, EXAFS scans with a 5 eV step and a 5 s integration time in the 7160–8000 eV range were obtained for normalization of the XANES spectra. Since in these experimental conditions the fluorescence intensity was proportional to the photoabsorption, the data were depicted as the quotient of the fluorescence intensity divided by the incident intensity as a function of X-ray energy. The data were processed using three steps. First, the scattering background was subtracted from the spectra. Second, the spectra were normalized to the fitted EXAFS heme iron atomic absorption oscillations in the 7160–8000 eV range (Bianconi *et al.*, 1984). Next, the derivative of the quotient of the fluorescence intensity divided by the incident intensity with respect to net energy was calculated by a method previously described (Poumellec *et al.*, 1988). The energy was referenced to E_0, which corresponded to the first maximum of the derivative absorption spectrum (Bianconi *et al.*, 1984). The root mean square of the error of energy was less than 0.2 eV.

The myoglobin samples were buffered in 100 mM potassium phosphate. The XANES reference spectra of native myoglobin were collected at pH 7 (2.4 mM aquometmyoglobin, Mb-H_2O) and at pH 11 (3.3 mM hydroxymetmyoglobin, Mb-OH^-). The XANES spectra of the 3.5 and 3.0 mM His64Tyr SW Mb solutions were recorded at pH 7 and 5.6, respectively. The heme iron electronic states were extracted from XANES spectra using the shape of its principal peaks.

RESULTS

Optical Spectra. Titration of the His64Tyr SW Mb between pH 3 and 9 exhibited three kinds of heme iron coordination states: denatured Mb with some free heme; Mb with heme iron bound to water; and Mb with heme iron bound to the distal tyrosine. At pH values less than 4.7, His64Tyr SW Mb became denatured. This pH value was close to the transition for the dissociation of the heme iron–proximal histidine bond (Giacometti *et al.*, 1977; Traylor *et al.*, 1983; Sage *et al.*, 1991). The heme dissociated from the protein was seen by the presence of a broad absorption band around 380 nm and the commensurate decrease of the Soret maximum absorption band. From pH 4.7 to 6, the increase in pH caused an increase

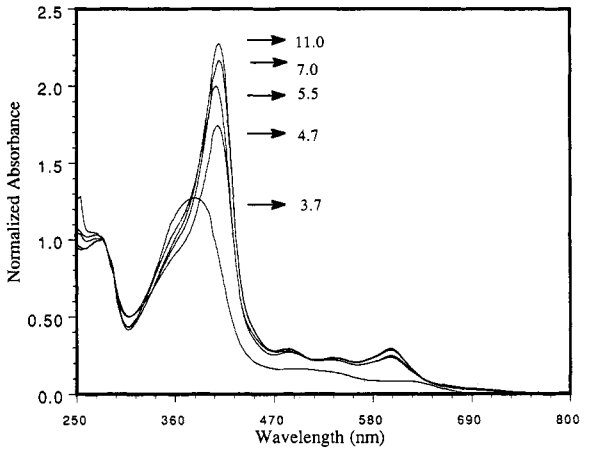

FIGURE 1: Absorption spectra of His64Tyr sperm whale myoglobin as a function of pH. Selected optical spectra of 10 mM solutions of His64Tyr SW Mb taken at 20 °C. The spectra were corrected for the background absorbance at 750 and 800 nm and were then normalized to the corrected absorbance at 280 nm. The decrease in pH caused a decrease in the absorbance values at 410, 486, 540, and 600 nm and an increase in the absorbance values at 250 nm. At pH values less than 4.0, there was a blue shift of the Soret band maximum indicative of the presence of free heme in solution.

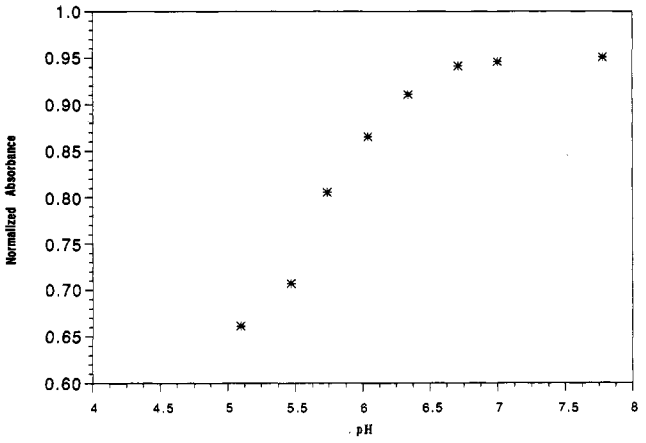

FIGURE 2: pH titration based on visible spectra of His64Tyr sperm whale myoglobin. The titration curve was based on absorbance values at 486, 540, and 600 nm. The calculation of the pK value relied upon data points from pH 5.0 to 11.0. The pK value associated with the heme iron coordination change was 5.6.

in the absorbance of the Soret band (410 nm) and visible spectrum, and a decrease in the absorbance value at 250 nm. Figure 1 shows these variations which indicate the formation of a heme iron–tyrosine bond. There were not any significant changes in the optical spectra from pH 6 to 11.0, indicating that there had been no changes in the heme iron electronic structure.

Analyses of the pH titration curves based on the visible bands (600, 540, 486, and 410 nm) yielded similar pK values. To avoid the problem of myoglobin denaturation, the titration curves were based on absorption values between pH 5 and 11. By fitting the data to eqs 1 and 2, the pK value of heme iron–tyrosine bond disruption was found to be 5.6 (see Figure 2).

Electron Spin Resonance Spectra. The ESR spectrum of WT aquometmyoglobin, pH 7, shows g values of high-spin six-coordinated heme iron (heme iron is bound to four pyrrole nitrogens, a proximal histidine imidazole nitrogen, and a water molecule). Figure 3 is an expansion of the $g \sim 6$ region which shows the major changes in the spectra after changes in pH. Below pH 6, the ESR spectrum of His64Tyr SW Mb showed high-spin axial heme iron coordination with g values of around

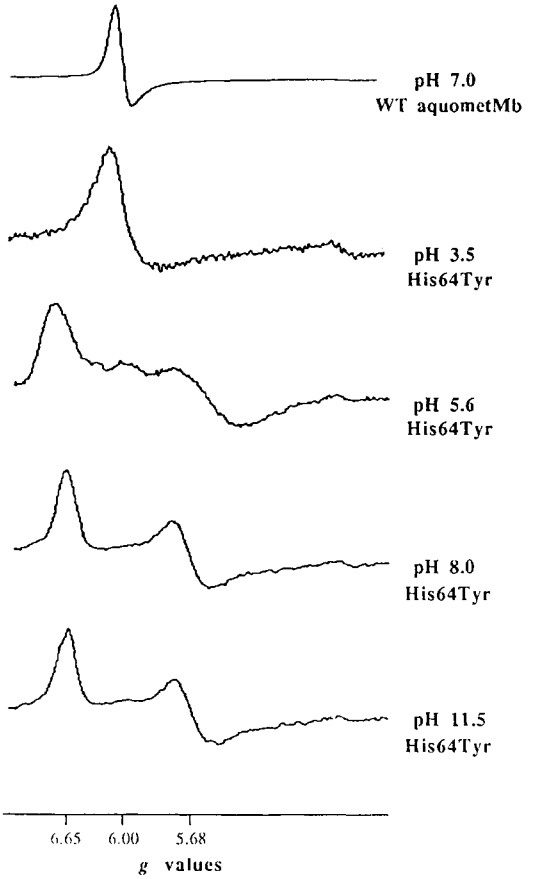

FIGURE 3: ESR spectra of His64Tyr sperm whale myoglobin at different pH values. Representative ESR first-derivative spectra of the $g = 7$ to the $g = 5$ region at different pH values are shown. Experimental details are given under Materials and Methods. The spectra were normalized to the difference of the largest and smallest data points. At low pH, the His64Tyr SW Mb mutant had a $g \sim 6$ peak similar to WT aquometmyoglobin. This was indicative of water binding to the heme iron. At pH values greater than 4, there was a higher concentration of rhombic $g \sim 6$ peaks characteristic of a heme iron–tyrosine bond. From pH 6.0 to 11.5, the ESR spectra had rhombic peaks suggestive of the heme iron–tyrosine bond. However from pH 8.0 to 11.5, low-spin signals from $g \sim 4$ increased greatly in intensity, indicating the presence of heme iron binding to hydroxide ion (data not shown).

6 and 2, which was reminiscent of metMb (Peisach *et al.*, 1971; Palmer, 1979). Because the rhombic component of the spectrum is at $g \sim 6$, it was likely that an important fraction of the heme iron binds a water molecule. This agreed with the optical spectra that give 50% of the heme iron–tyrosine bond disrupted at pH 5.6. Between pH 6 and 9, the His64Tyr SW Mb spectra have rhombically split high-spin heme iron signals in the $g \sim 6$ region. This protein exhibits g values of 6.63, 5.31, and 1.98 at pH 7.0, which are similar to those reported for Hb M Saskatoon, g values of 6.65, 6.0, 5.35, 4.3, and 2.0 (Hayashi *et al.*, 1969; Egeberg *et al.*, 1990).

XANES Spectroscopy. The X-ray absorption iron K-edge reveals the electronic transitions from the 1s level to the lowest unoccupied atomic states (Bianconi, 1980). The effects of different ligands binding to the heme iron atom can be characterized by comparative analyses of the K-edge shapes of heme proteins (Morante *et al.*, 1983; Pin *et al.*, 1985). A heme iron electronic reorganization, subsequent to spin redistribution, is observable to about 20 eV, corresponding to the principal peak(s) of the derivative of the XANES spectrum (Oyanagi *et al.*, 1987; Pin *et al.*, 1989).

In Figure 4, the heme iron XANES spectrum and the first-

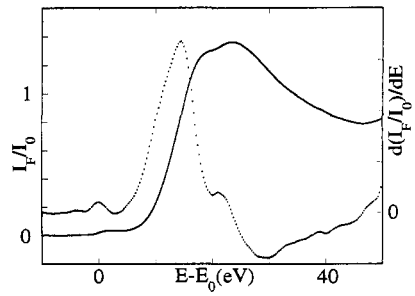

FIGURE 4: XANES of wild-type sperm whale myoglobin. The heme iron K-edge spectrum was collected on 2.4 mM WT SW Mb in 100 mM potassium phosphate buffer at pH 7.0 and at 19 °C. The left axis corresponding to the XANES experimental spectrum (solid line) represents the ratio of the iron fluorescence, I_f, divided by the incident X-ray intensity, I_0 (I_f/I_0). The right axis shows the units for the derivative (dotted line), $d(I_f/I_0)/dE$, of the XANES spectrum. The peak positions of the derivative spectrum were 14.5 eV for the principal peak and 21.0 eV for the second peak. The full width at half-maximum (FWHM) value of the principal peak was 7.25 eV.

derivative spectrum of wild-type recombinant sperm whale myoglobin at pH 7 exhibited the typical pattern observed for native Mb-H_2O (Oyanagi *et al.*, 1987). The behaviors of preedge and edge characteristics, the shape, and the peak positions of the XANES first-derivative spectra (14.5 eV for the principal peak and 21.0 eV for the second) were the same. The full width at half-maximum value (FWHM) of the principal peak of the derivative was 7.25 eV and was characteristic of a strongly high-spin heme iron state as previously determined for natural aquometmyoglobin (Iizuka & Kotani, 1969). Thus, the wild-type recombinant myoglobin, pH 7.0, was identical with the native myoglobin where a water molecule is the ligand on the heme iron.

The heme iron XANES spectrum and the first-derivative spectrum of His64Tyr SW Mb at pH 7.0 are presented in Figure 5A. The edge behavior had the characteristic features of the native $MbOH^-$ (Figure 6). The derivative spectrum exhibited a shoulder at ca. 20 eV which is indicative of a hydroxyl ion as the heme iron sixth ligand (Oyanagi *et al.*, 1987). The position of the derivative maximum was 14.0 eV, and the FWHM value was 8.0 eV. These values were similar to those of $MbOH^-$ (14.5 and 7.5 eV). The major difference between His64Tyr SW Mb and hydroxymetmyoglobin was that the preedge intensity for His64Tyr SW Mb was taller than that of hydroxymetmyoglobin. This increase was probably derived from the increase of the weak intensity of the forbidden electronic transition of 1s to 3d shells when the heme iron was bound to a stronger field ligand and the environment surrounding the heme iron became more compact (Pin *et al.*, 1982). These results implied that the His64Tyr SW Mb has a hydroxyl-like group bound to the heme iron. This hydroxyl-like group implicated in heme iron binding should be the phenol group of the distal tyrosine.

A comparison of the XANES derivative spectra of His64Tyr SW Mb at pH 5.6 and at pH 7.0 revealed some changes (Figure 5A,B). Although the shapes of the spectra were similar when the pH was lowered from 7.0 to pH 5.6, the intensity of the XANES preedge spectrum was higher, the FWHM value broadened from 8.0 to 9.5 eV, and the peak position of the first-derivative peak was shifted from 14.0 to 13.0 eV. This 1 eV change was significantly larger than the root mean square error of the energy (<0.2 eV). Since the FWHM value increases when the high-spin population increases (Oyanagi *et al.*, 1987; Pin *et al.*, 1989), His64Tyr SW Mb had an increased population of high-spin character when the pH decreased.

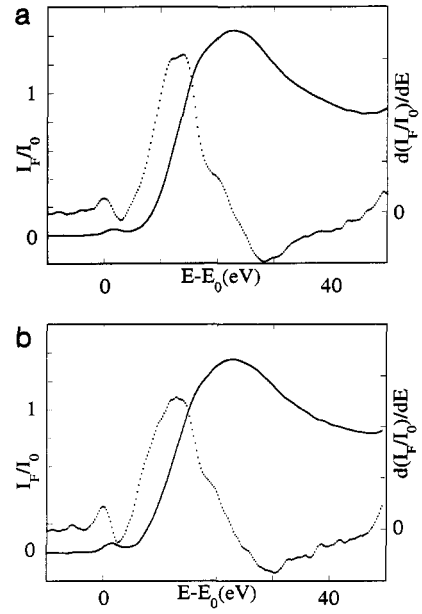

FIGURE 5: XANES of His64Tyr sperm whale myoglobin. The heme iron K-edge spectra were collected at two different pH values: (A) 3.5 mM His64Tyr SW Mb in 100 mM potassium phosphate buffer at pH 7.0 at 19 °C; (B) 3.0 mM His64Tyr SW Mb in 100 mM potassium phosphate buffer at pH 5.6 and at 19 °C. The left axis corresponding to the XANES experimental spectrum (solid line) represents the ratio of the heme iron fluorescence I_f divided by the incident X-ray intensity I_0 (I_f/I_0). The right axis shows the units for the derivative (dotted line) $d(I_f/I_0)/dE$ of the XANES spectrum. The positions of the peaks of the first-derivative spectra were (A) 14.0 eV and (B) 13.0 eV. The respective FWHM value was (A) 8.0 eV and (B) 9.5 eV.

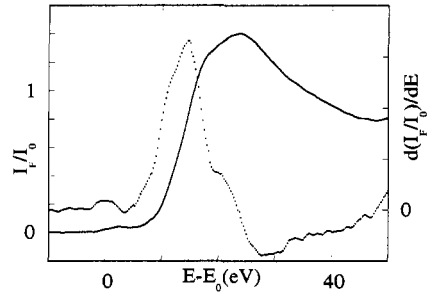

FIGURE 6: XANES of native sperm whale hydroxymetmyoglobin. The heme iron K-edge spectrum was collected on 3.3 mM myoglobin in 100 mM potassium phosphate buffer at pH 11 at 19 °C. The left axis corresponding to the XANES experimental spectrum (solid line) represents the ratio of the heme iron fluorescence I_f divided by the incident X-ray intensity I_0 (I_f/I_0). The right axis shows the units for the derivative (dotted line) $d(I_f/I_0)/dE$ of the XANES spectrum. The peak position of the derivative spectrum was 14.5 eV. The FWHM value was 7.5 eV.

DISCUSSION

Crystallographic analyses of abnormal hemoglobins M show that the tyrosine at position 64 is directly bound to the iron atom (Pulsinelli *et al.*, 1973). The similarity of the optical absorption, electron spin resonance, and resonance Raman spectra of the His64Tyr SW Mb to Hb M Boston and Hb M Saskatoon suggests that its heme iron coordination is similar to that of the other two Hb M mutants (Egeberg *et al.*, 1990). However, in each of the prior discussions, the tyrosine phenolate ion ($Fe–O^-_\Phi$) is considered to be the ligand to the heme iron. Molecular dynamics simulations of this mutant confirmed the possibility that tyrosine-64 was inaccessible to solvent and remained within the heme pocket. A model of the heme pocket of His64Tyr SW Mb is shown in Figure 7.

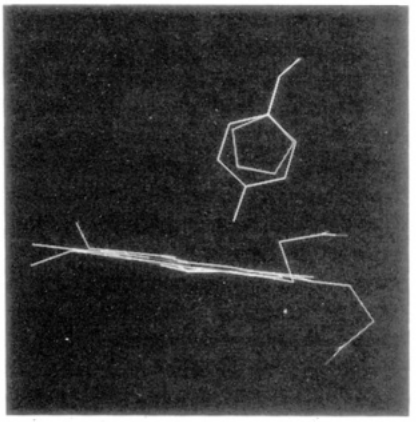

FIGURE 7: Comparison of the heme pocket of wild-type sperm whale myoglobin and a simulation of the heme pocket of His64Tyr sperm whale myoglobin mutant using the MANOSK molecular graphics program (Cherfils *et al.*, 1988).

XANES spectroscopy of His64Tyr SW Mb shows that the heme iron is bound to a hydroxyl-like group, suggesting that the phenol oxygen of the distal tyrosine is still protonated. The electronic arrangements of the oxygen atom of a water molecule and a tyrosine phenol group are similar in that both are very polar. However, only the oxygen atom in the H_2O molecule has a symmetric environment. The oxygen in the tyrosine phenol group (Φ-OH) experiences two inductive effects: a repulsive effect due to the phenyl group (Φ) and an attractive effect due to the proton. This electronic delocalization on the oxygen atom can explain the linkage of the Φ-OH to the heme iron with binding between the oxygen and the heme iron. We have observed the increase of the heme iron high-spin population of the mutated myoglobin when the pH decreases from 7 to 5.6. A pH change could produce a modulation of the inductive characters of Φ-OH groups of tyrosine E7 which in turn modifies the electronic delocalization on the oxygen atom. Thus, the ionic character of Fe–OH_Φ binding evolves with the pH of the solution with a commensurate change in the heme iron high-spin population.

The pH and ESR titrations of His64Tyr SW Mb monitored the effect of pH on the heme iron ligands. Since the signals characteristic of high-spin heme iron–tyrosine ligation were monitored, pH titration characterized this heme iron–tyrosine ligand bond. The pH titrations of the optical spectra suggested that the heme iron coordination change occurs with a pK of 5.6. At low pH, the similarity of the ESR spectra to those of native SW Mb suggested that the heme geometry is similar to that of aquometmyoglobin. In other words, proximal histidine-93 is still bound to the heme iron without the bond between the distal tyrosine and the heme iron. The broad width of the rhombic component ($g \sim 6$) suggested that the heme iron did not bind the distal tyrosine but rather a water molecule in this pH range.

The phenol group of free tyrosine has a pK_a value of 10.5 (Stryer, 1988). Hence, the assertion that the sixth heme ligand of His64Tyr SW Mb is a phenolate ion requires the heme pocket to have drastically altered the intrinsic tyrosine phenol group pK_a of 10.5. Often basic residues are required to cause such shifts in the pK_a (Stites *et al.*, 1991). Since the tyrosine side chain is not significantly larger than a histidine side chain and is bound to the heme iron, we assume that the tyrosine ring is in close proximity to the original position of the histidine-64 ring in wild-type SW Mb. Of the three basic residues near residue 64, only Arg 45 is poised to interact with the distal Tyr64 (Takano, 1977; Kuriyan *et al.*, 1986); the other two residues, Lys62 and Lys63, point away from the heme pocket. Typically, in the environment of such polar residues, the pK_a shifts are not by more than 3 units away from their intrinsic values. For instance, the His64 imidazole nitrogens have a pK_a value of about 4.4 (Li & Spiro, 1988). Since the intrinsic pK_a of free histidine is about 6.0, this pK_a value shows that the polarity of the heme pocket makes the imidazole nitrogen deprotonate more easily. In the crystalline SW Mb structures, the Arg45 ζ nitrogens are believed to form a hydrogen bond network with water and sulfate ions to the His64 imidazole $N_\delta 1$ nitrogen. Hence, the arginine may lower the potential of deprotonation of the imidazole nitrogen. Since the imidazole nitrogen is a weaker base than the phenol oxygen, one would expect the phenol oxygen to be more difficult to deprotonate than the histidine imidazole nitrogen. The presence of an electrophilic heme iron could also decrease the pK_a value of this residue (Spiro, 1983). Preliminary efforts, using the program DELPHI on an energy-minimized sperm whale metMb mutant, to simulate the pK_a change of the His64Tyr SW Mb mutant were unsuccessful because of the difficulty of parameterizing the atoms in the heme group (Gilson & Honig, 1988).

After the transition evident from the optical titrations at pH 5.6, no additional transitions were seen up to pH 11. There are no obvious transitions associated with the deprotonation of the phenol oxygen when it is bound to the heme. However, it is unclear whether the deprotonation of the phenol oxygen can be seen either by electron spin resonance or by optical spectra (Smith & Williams, 1970; Peisach *et al.*, 1971; Peisach & Gersonde, 1977). Preliminary ^1H high-spin NMR data did not show the presence of the phenol hydrogen (Chiu and Sligar, unpublished results). Presumably, the zero-field coupling constant of the phenol hydrogen atom is similar to that of the water hydrogen atoms. These water protons are expected to have broad line widths, simulated to be several kilohertz wide, which make them difficult to detect by NMR (Gerd La Mar, private communication).

For horse heart His6e(E7)Tyr myoglobin, it was also shown that the sixth ligand of the heme iron was water at pH 4 and the distal tyrosine phenol group at pH 7 (Tang *et al.*, 1991). This observation confirms our ESR and XANES results. When the pH decreases to pH 4, the ionic character of Fe–OH_Φ binding increases, causing weaker Fe–OH_Φ bonding and thus allowing the coordination of another ligand, a water molecule in this case (Nagai *et al.*, 1989). The pK value of His64Tyr SW Mb is 1 pH unit different from the value of 4.5 determined for the recombinant horse His64Tyr metMb (Tang *et al.*, 1991). There are 13 amino acid differences between horse and sperm whale myoglobin, many of which are found in the interior of the protein. Presumably, the differences in the pK values between the axial tyrosine–heme iron ligation of horse and SW Mb were caused from these interior amino acid differences (Gilson & Honig, 1988).

ACKNOWLEDGMENT

We are very much indebted to technicians and engineers of LURE and the Laboratoire de l'Accélérateur Linéaire (Orsay, France) for running DCI for synchrotron radiation. We thank Dr. O. Sire for his assistance in modeling and analyzing the myoglobin molecular structures, and Dr. J.-P. Mornon and Dr. M.-C. Vaney for their help in using MANOSK graphics in the Laboratoire de Minéralogie–Cristallographic, Universités Paris VI et VII. We thank Dr. Gerd La Mar, Dr. Peter Debrunner, Dr. Phil Nyman, and Dave Benson for helpful discussions.

REFERENCES

Amiconi, G., Santucci, R., Coletta, M., Congiu-Castellano, A., Giovanelli, A., Dell'Ariccia, M., Della Longa, S., Barteri, M., Burattini, E., & Bianconi, A. (1989) *Biochemistry 28*, 8547–8553.

Beck von Bodman, S., Schuler, M. A., Jollie, D. R., & Sligar, S. G. (1986) *Proc. Natl. Acad. Sci. U.S.A. 83*, 9443–9447.

Bianconi, A. (1980) *Appl. Surf. Sci. 6*, 392–418.

Bianconi, A., Congiu-Castellano, A., Dell'Arricia, M., Giovanelli, A., Durham, P. J., Burattini, E., & Barteri, M. (1984) *FEBS Lett. 178*, 165–170.

Bianconi, A., Congiu-Castellano, A., Durham, P. J., Hasnain, S. S., & Phillips, S. (1985) *Nature (London) 318*, 685–687.

Cherfils, J., Vaney, M. C., Morize, I., Surcouf, E., Colloch, N., & Mornon, J. P. (1988) *J. Mol. Graphics 6*, 155–160.

Choi, S., & Spiro, T. G. (1983) *J. Am. Chem. Soc. 105*, 3683–3692.

Egeberg, K. D., Springer, B. A., Martinis, S. A., Sligar, S. G., Morikis, D., & Champion, P. M. (1990) *Biochemistry 29*, 9783–9791.

Giacometti, G. M., Traylor, T. G., Ascenzi, P. A., Brunori, M., & Antonini, E. (1977) *J. Biol. Chem. 252*, 7447–7448.

Gilson, M., & Honig, B. (1988) *Proteins: Struct., Funct., Genet. 4*, 7–18.

Hayashi, A., Suzuki, T., Imai, K., Morimoto, H., & Watari, H. (1969) *Biochim. Biophys. Acta 194*, 6–15.

Iizuka, T., & Kotani, M. (1969) *Biochim. Biophys. Acta 181*, 275–286.

Jaklevic, J., Kirby, J. A., Klein, M. P., Robertson, A. S., Brown, G. S., & Eisenberger, P. (1977) *Solid State Commun. 23*, 679–682.

Jaklevic, J. M., Giauque, R. D., & Thompson, A. C. (1987) *Anal. Chem. 60*, 482–484.

Kuriyan, J., Wilz, S., Karplus, M., & Petsko, G. A. (1986) *J. Mol. Biol. 192*, 133–154.

Li, X.-Y., & Spiro, T. G. (1988) *J. Am. Chem. Soc. 110*, 6024–6033.

Morante, S., Cerdonio, M., Vitale, S., Congiu-Castellano, A., Vaciago, A., Giaconnetti, G. M., & Incoccia, L. (1983) *Chem. Phys. Ser. 27*, 352–354.

Morse, P. D. (1987) *Biophys. J. 51*, 440a.

Oyanagi, H., Iizuka, T., Matsushita, T., Saigo, S., Makino, R., & Ishimura, Y. (1986) *J. Phys. 47*, C18-1147-1150.

Oyanagi, H., Iizuka, T., Matsushita, T., Saigo, S., Makino, R., & Ishimura, Y. (1987) in *Biophysics Series* (Bianconi, A., & Congiu-Castellano, A., Eds.) Vol. 2, pp 99–106, Springer-Verlag, New York.

Palmer, G. (1979) in *The Porphyrins*, Vol. IV, Chapter 6, p 325, Academic Press, Inc., New York.

Peisach, J., & Gersonde, K. (1977) *Biochemistry 16*, 2539–2545.

Peisach, J., Blumberg, W. E., Ogawa, S., Rachmilewitz, E. A., & Oltzik, R. (1971) *J. Biol. Chem. 246*, 3342–3355.

Penner-Hahn, J. E., & Hodgson, K. O. (1989) in *Physical Bioinorganic Chemistry Series* (Lever, A. B. P., & Gray, H. B., Eds.) Vol. 4, pp 275–281, VCH Publishers, New York.

Pin, S., Alpert, B., & Michalowicz, A. (1982) *FEBS Lett. 147*, 106–110.

Pin, S., Valat, P., Cortès, R., Michaelowicz, A., & Alpert, B. (1985) *Biophys. J. 48*, 997–1001.

Pin, S., Le Tilly, V., Alpert, B., & Cortès, R. (1989) *FEBS Lett. 242*, 401–404.

Poumellec, B., Cortès, R., & Marcelet, F. (1988) *J. Appl. Crystallogr. 21*, 209.

Press, W. H., Flannery, B. P., Tenkolsky, P. A., & Vetterling, W. T. (1986) in *Numerical Recipes*, Cambridge University Press, Cambridge, UK.

Pulsinelli, P. D., Perutz, M. F., & Nagel, R. L. (1973) *Proc. Natl. Acad. Sci. U.S.A. 70*, 3870–3874.

Raphael, A. L., & Gray, H. B. (1991) *J. Am. Chem. Soc. 113*, 1038–1040.

Sage, J. T., Morikis, D., & Champion, P. M. (1991) *Biochemistry 30*, 1227–1237.

Sligar, S. G., Egeberg, K. D., Sage, J. T., Morikis, D., & Champion, P. M. (1987) *J. Am. Chem. Soc. 109*, 7896–7897.

Smith, D. W., & Williams, R. J. P. (1970) *Struct. Bonding 7*, 1–45.

Spiro, T. G. (1983) in *Iron Porphyrins* (Lever, A. B. P., & Gray, H. B., Eds.) Vol. 2, p 89, Addison-Wesley, Reading, MA.

Spiro, T. G., Strong, J. D., & Stein, P. (1979) *J. Am. Chem. Soc. 101*, 2648–2655.

Springer, B. A., & Sligar, S. G. (1987) *Proc. Natl. Acad. Sci. U.S.A. 84*, 8961–8965.

Stites, W. E., Gittis, A. G., Lattman, E. E., & Shortle, D. (1991) *J. Mol. Biol. 221*, 7–14.

Stryer, L. (1988) in *Biochemistry* pp 148–150, Freeman, New York.

Takano, T. (1977) *J. Mol. Biol. 110*, 537–568.

Tang, H., Chance, B., Mauck, C., Powers, L., Reddy, K. S., & Smith, M. (1992) *Biophys. J. 61*, A213.

Tourillon, G., Guay, D., Lemonnier, M., Bartol, F., & Badeyan, M. (1990) *Nucl. Instrum. Methods Phys. Res., Sect. A A294*, 382–390.

Traylor, T. G., Deardurff, L. A., Coletta, M., Ascenzi, P., Antonini, E., & Brunori, M. (1983) *J. Biol. Chem. 258*, 12147–12148.